OPF Techniques for Real-Time Active Management of Distribution Networks

James G. Robertson, Gareth P. Harrison, *Senior Member, IEEE*, and A. Robin Wallace

***Abstract*—This paper presents a method for real-time active network management (ANM) control to maximize network-wide energy yield in constrained networks. Coordinated scheduling of renewable distributed generation (DG) and distribution network control assets can limit DG curtailment and significantly increase energy yield and economic performance of DG. Here, an optimal power flow approach has been developed for real-time online scheduling of network control settings to better integrate high levels of temporally and spatially variable DG from renewable energy resources. Results show that the real-time prescription of ANM control settings provides a feasible alternative to network reinforcement under the existing passive management philosophy.**

***Index Terms*—Active network management, distributed generation, optimal power flow, distribution management system.**

I. Introduction

CONNECTING increasing levels of temporally and spatially varying renewable distributed generation (DG) within the capabilities of the existing distribution networks is a technical and economic challenge for distribution network operators (DNOs) [1]. To accommodate enhanced levels of DG in distribution networks conventional 'fit-and-forget' approaches are being evolved into 'connect-and-manage' systems using Active Network Management (ANM) [2]. The advantages of real-time active network control and their coordination through advanced communications, is strongly supported as a means of integrating new network participants while exploiting the potential of existing network assets [3], [4]. While the actual implementation of ANM by DNOs will depend on the economic and regulatory framework, the technical feasibility of the network to accept and support high DG penetration levels needs to be addressed.

Initial projects that focus on independent DG control strategies to increase connectable capacity have illustrated considerable benefits of ANM. Existing research [5] proposed strategies for localised voltage regulation through intelligent reactive power dispatch as a means of mitigating the voltage rise constraints. An extension to this work included the localised constrained-dispatch of active power to address voltage rise beyond the reactive power capability of the DG as well as the management of overhead line and transformer flows [6]. More 'centralised' solutions have been developed to relieve voltage and thermal overloading restrictions on DG capacity. For example, the Orkney ANM scheme [4] performs real-time monitoring of loading at strategic boundaries and systematically curtails production from DG on a last-in, first-off (LIFO) basis when power flows could cause violation.

Optimal Power Flow (OPF) has been used extensively for economic dispatch of constrained transmission systems [7]. Recently OPF entered the distribution network literature for both planning and dispatch; this has a more 'technical' rather than 'economic' focus to fit with the unbundled regulatory environment for DNOs. Application of the OPF to evaluating hosting capacity and the impact of ANM techniques [8], suggests that coordinated scheduling of DG and active network assets can enhance renewable capacity and increase DG energy yield. Boehme *et al.* [9] apply OPF to optimally curtail renewable DG to avoid thermal and voltage overloads while [10] deploys OPF for thermal constraint management.

DNOs are currently reluctant to deploy autonomous ANM concepts or rely on third party network regulation due to limited knowledge on the system interactions and potential impact on network operation. To actively manage multiple system constraints, it is necessary to coordinate and validate each control protocol to ensure that control actions are not unnecessarily replicated and that the scheme exhibits safe and satisfactory resolution of the control sequences.

Here, a new application and real-time formulation of the AC OPF is presented that employs ANM of DG active and reactive power and coordinated voltage control to maintain the voltage and thermal limits in constrained distribution networks. A real-time simulation framework incorporating the new OPF as its dispatch system allows visualisation of the time-dependent impacts of measurements, communication and control sequences in a realistic fashion. Operating on a 5-minute control cycle, application to a section of renewable-rich distribution network clearly identified that variable power flows and the actions of the control elements resulted in 'residual' variations within the control cycles leading to constraint violations. The incorporation of a new 'smoothing' mechanism within the OPF was found to substantially improve voltage and power flow compliance and stabilise operation.

This paper is structured as follows. Section II presents the formulation of the real-time ANM OPF and simulation environment. Section III presents two case studies investigating

Manuscript received February 11, 2016; revised June 27, 2016 and September 13, 2016; accepted October 24, 2016. Date of publication December 7, 2016; date of current version August 17, 2017. This work was supported by the Engineering and Physical Research Council under Grant EP/F061242/1 and Grant EP/I035773/1. Paper no. TPWRS-00228-2016.

The authors are with the Institute for Energy Systems, School of Engineering, University of Edinburgh, Edinburgh EH9 3DW, U.K. (e-mail: J.Robertson@ed.ac.uk; Gareth.Harrison@ed.ac.uk; Robin.Wallace@ed.ac.uk).

Color versions of one or more of the figures in this paper are available online at http://ieeexplore.ieee.org.

Digital Object Identifier 10.1109/TPWRS.2016.2624985

0885-8950 © 2016 IEEE. Translations and content mining are permitted for academic research only. Personal use is also permitted, but republication/redistribution requires IEEE permission. See http://www.ieee.org/publications_standards/publications/rights/index.html for more information.

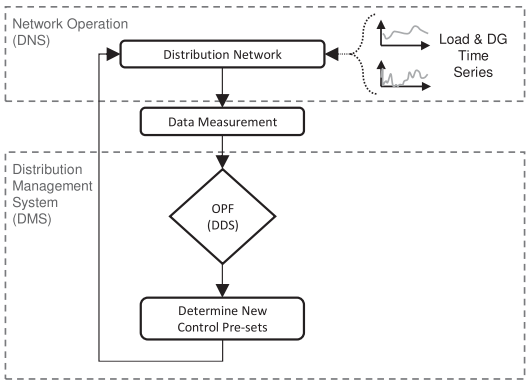

Fig. 1. Real-time simulation architecture.

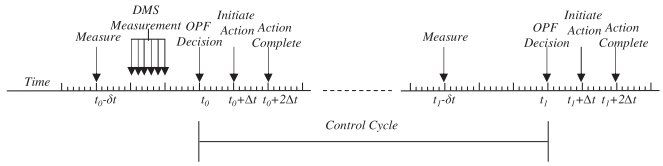

Fig. 2. Control interval and DG control practice.

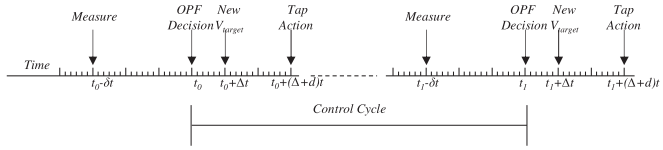

Fig. 3. OLTC transformer control practice.

application of the real-time OPF on generic models of the UK medium voltage distribution network. Sections IV and V discuss and draw conclusions.

II. Problem Formulation

A. Framework for Real Time Simulation

The solution architecture and software environment [11] were developed to perform time-sequential power flow analysis simulating 'real-time' network operation across successive steady state intervals. The model architecture, shown in Fig. 1, has two interfaced elements: (i) a distribution management system (DMS) within which a range of management approaches can be articulated; and (ii) a distribution network simulator (DNS) that translates commands within specific infrastructure within the 'proxy' distribution network. A key part of the DMS is the distribution dispatch system (DDS) optimisation platform which uses the OPF algorithm to determine the required network settings.

This system provides the opportunity to program and interpret new formulations of OPF without acting directly on the control settings in the power flow. In addition, it allows the active regulation of individual DG and network asset controllers to be modelled explicitly in the power flow solution so that the control interactions and network response under 'connect-and-manage' strategies can be observed.

Variable power flow conditions are modelled by time series profiles of generation and demand. The time series input data are fed exclusively to the power flow solutions of the 'proxy' distribution network. Sampling of 'real time' load and generation values, as well as prevailing network conditions, is carried out by the distribution management system and input into the OPF. This mimics operation of a realistic system.

The OPF is formulated in the AIMMS optimisation modelling environment using the CONOPT 3.14A nonlinear solver. Plug-and-play of the OPF into the software environment via the COM interface allows the OPF to be implemented online. OpenDSS [12] is the power flow engine used to simulate the 'proxy' distribution network.

B. Control Flow and Operating Margins

The process of simulating the operation and control of the network is a continuous repetitive cycle of activities, as Fig. 2 shows. To facilitate observation of variations in the network state and the interaction of control schemes, the 'proxy' distribution network is simulated using steady-state power flow at short time intervals, in this case 5-seconds. It should be noted that the communication, analysis and implementation time delays are included to be representative of real settings. The network controls are scheduled on a longer cycle, in this case a 5-minute control interval is used. All actions are expressed relative to the availability of new set-points from the OPF, t_0. The time sequence is as follows:

Time $t_0 - \delta t$: 'measurement' of the network state including resource availability and demand loading level. This is achieved by recording the previous outputs of the power flow solution and occurs δt prior to the cycle interval and is designed to represent communication and analysis delays in the metering and communications infrastructure and in the DMS. For illustration, the delay is assumed to be 90-seconds.

Time t_0: The network state is fed as input to the OPF DDS which executes and provides new control and DG dispatch set-points. The execution time is very short compared to operational timescales.

Time $t_0 + \Delta t$: The set-points are passed by the DMS to the 'proxy' network for implementation. The Δt delay is imposed by communications delays and is assumed to be 30-seconds.

Time $t_0 + 2\Delta t$: Once the transition from existing state is initiated the control actions of each network component vary according to their respective control practices. All actions are complete by time $t_0 + 2\Delta t$. For DG active power output, the ramp rate applied to newly prescribed control setting occurs linearly across each of 5-s simulation steps in the interval Δt. This is representative of the real-time rate-of-change of production instigated by ANM schemes. Changes to the DG reactive power dispatch occurs in tandem with the active power dispatch (as DG operates in power factor control mode), but the change occurs instantaneously (within the 5-seconds simulation step). Tap-changing OLTCs are assumed to embody standard operating practice of a (typically) 60-seconds delay prior to the tapping action, as illustrated in Fig. 3.

The impact and implications of the measurement and communications delays are considered within the case studies.

In this concept the OPF technique is used to dispatch individual target set-points for local control assets; these then invoke changes in local infrastructure as opposed to enacting direct control of local controllers. With active control dispatch operating on a longer time cycle than the corrective control actions of local network controllers, time delays in measurement, communication and control actions do not directly influence the time sequential steady-state solutions of the OPF. The impact of delays and ramp-rates is used to identify the real time system consequences of active network dispatch. A key contribution of this work is the quantification of 'residual' system variation between the steady-state solutions of the OPF and the realisation of system control switching enacted by local controllers. The term 'operating sensitivity' refers to the inherent residual variability of network state and control variables in real time, arising from system deadbands, ramp-rates and communication time delays.

C. Distribution Dispatch: AC OPF Formulation

The dispatch of the network and DG set-points is carried out by a bespoke AC OPF formulation based on an earlier multi-period OPF [8] but substantially altered for use in a 'real-time' setting and to improve its operational characteristics. It is designed to operate at defined intervals in discrete time, using data on generation output and demand levels 'sampled' from the network.

To represent the DNO responsibility to maximise access to the network, the OPF objective function primarily maximises network-wide energy yield over time by minimising the curtailment of DG active power. When introduced in a fairly 'standard' OPF this may lead to selection of operating positions in successive time periods that are quite different as a result of the numerical similarity of the objective function value despite differing inputs and control values. This solution was shown to be vulnerable to residual variation in the network. To counteract this effect a secondary penalty function is employed within the objective to minimise deviation on system regulated bus voltages. The final objective function is:

$$Min \sum_{g \in G} p_g^{curt} + \sum_{b \in B} (V_{b,reg} - V_{b,reg}^{\text{target}})^2 \tag{1}$$

where p_g^{curt} is the active power curtailment of DG *g* (set *G*), $V_{b,reg}$ is the regulated network voltage settings at bus *b* and $V_{b,reg}^{\text{target}}$ is the favoured operational target set-points. Curtailment and voltage levels are evaluated in per-unit terms and intuitively scaled such that they do not occupy the same physical meaning in the solution space and can therefore be evaluated directly. The addition of a 'minimum deviation' term stabilises successive solutions of the OPF and identifies one solution to an identified multifaceted problem of dispatch and mitigation of very short term residual variation. It serves to improve the continuity of control set-points on voltage-regulated buses by penalising changes of little or no value at each successive control period. To demonstrate the value of the 'minimum deviation' arrangement, a 'standard' objective function was also examined as a comparator:

$$Min \sum_{g \in G} p_g^{curt} \tag{2}$$

Beyond this, the OPF formulations are otherwise identical.

The optimisation is subject to a range of normal constraints. These include active and reactive nodal power balance:

$$\sum_{l \in L \,|\, \beta_l^{i,j} = b} p_b^l + d_b^P \eta = \sum_{g \in G \,|\, \beta_g = b} \left[p_g \omega - p_g^{curt} \right] + \sum_{x \in X \,|\, \beta_g = b} p_x \tag{3}$$

$$\sum_{l \in L \,|\, \beta_l^{i,j} = b} q_b^l + d_b^Q \eta = \sum_{g \in G \,|\, \beta_g = b} \left[p_g \omega - p_g^{curt} \right] \times \tan(\phi_g) + \sum_{x \in X \,|\, \beta_g = b} q_x \tag{4}$$

where p_g is installed DG capacity; $d_b^{(P,Q)}$ denotes peak active and reactive demand at bus *b* (set *B*), $(p,q)_x$ are interconnector flows, $(p,q)_b^l$ are the active and reactive power injections at the ends of each branch (denoted *i* and *j*); and ϕ_g the DG power factor angle. At each discrete time interval the per-unit level of resource availability relative to nominal capacity is ω_g and η is the per-unit demand level.

The complex power injections at the ends of each branch are determined in terms of voltage levels and angles by the standard Kirchhoff's voltage law formula. In the case of transformers, the primary voltage (V_i) must be divided by the transformer tap ratio, τ_l. For active management of the OLTCS and voltage regulators the tap ratio is constrained within the limits of each transformer:

$$\tau_l^- \leq \tau_l(t) \leq \tau_l^+ \tag{5}$$

Bus voltages V_b are constrained within maximum and minimum levels $V_b^{(+,-)}$:

$$V_b^- \leq V_b \leq V_b^+, \forall b \in B\,. \tag{6}$$

While UK regulations allow voltages of $\pm 6\%$ of nominal at 11 and 33kV, a more conservative envelope of $\pm 5.5\%$ is employed to mitigate some of the real time residual voltage variation due to operating sensitivity in the 'proxy' distribution solution.

The apparent power flow limit of each transformer and line *l* ($\forall l \in L$) is limited to the thermal rating s_l:

$$(p_{(i,j)}^l)^2 + (q_{(i,j)}^l)^2 \leq (s_l)^2 \tag{7}$$

The power flow thresholds were set at rated capacity as small short term overloading of network assets was considered acceptable.

Import/exports limit at the network boundaries also apply:

$$\left.\begin{aligned} -p_x^+ \leq p_x \leq p_x^+ \\ -q_x^+ \leq q_x \leq q_x^+ \end{aligned}\right\} \quad \forall x \in X \tag{8}$$

D. ANM Control Techniques

Three control techniques are included in the OPF scheme: Curtailment; variable Power Factor Control (PFC) and

Coordinated Voltage Control (CVC). This assumes that DNOs are capable of controlling existing network assets and centrally dispatching DG active and reactive power output.

Curtailment of the DG active power output can be used to regulate network power flows and voltage levels within acceptable regimes, according to:

$$0 \leq p_g^{curt} \leq p_g \omega_g \ \forall g \in G \tag{9}$$

Power curtailment is modelled as a simple reduction of production. To maximise energy yield from DG, the set-point issued to the distribution network simulator is a per-unit transformation of the resource-dependent power output. Therefore the set-point issued to the DG is a calculated measure of anticipated output based on forecasted resource not a portion of maximum sustainable power output.

Currently, the obligation on DGs to provide network support and ancillary services is dependent on plant size, technology and connection contracts. Here, all DG plants are assumed to have the technological capability and are available to the OPF to provide network support. This is in the form of variable power factor control which regulates the voltage level at the point of connection for a DG by actively adjusting the DG power factor angle to absorb or inject reactive power:

$$\phi_g^- \leq \phi_g \leq \phi_g^+ \tag{10}$$

Steady-state voltage targets traditionally allow OLTCs and voltage regulating transformers to maintain voltage levels under variable load patterns. With CVC this principle extends to allow dynamic control of target voltage levels to meet the evolving need of distribution networks

$$V_{b,reg}^- \leq V_{b,reg} \leq V_{b,reg}^+ \tag{11}$$

E. Forecasting

With the system operating with a short 5 minute control interval, there may only be modest benefit from short-term forecasting. As such, persistence forecasting is used which means that the value sampled at the start of the period applies for the duration of the control cycle. The generation output and demand level are sampled along with other network parameters at the 'measurement' stage of the cycle, i.e. 90s ahead of the set-point time t_0.

III. Case Study

The case study demonstrates the operation and effectiveness of the real-time ANM OPF control algorithms in two UK Generic Distribution System (GDS) [13] networks. The first is a simplified version of the second, using a single DG and a simple set of constraints. The second employs multiple DGs and resources and a more extensive set of constraints. Both networks were used in [8] and allow some comparison between planning and operational situations.

Both case studies employ the same generation and demand datasets. Fig. 4 shows the representative demand pattern and generation profiles for wind and tidal generation for the 24-hour test period. These are based on one second data from individual

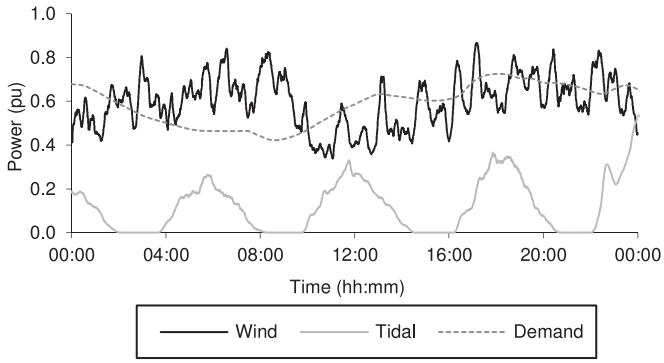

Fig. 4. 24-hour renewable energy resource generation and demand profiles (p.u. of installed capacity and annual winter peak demand).

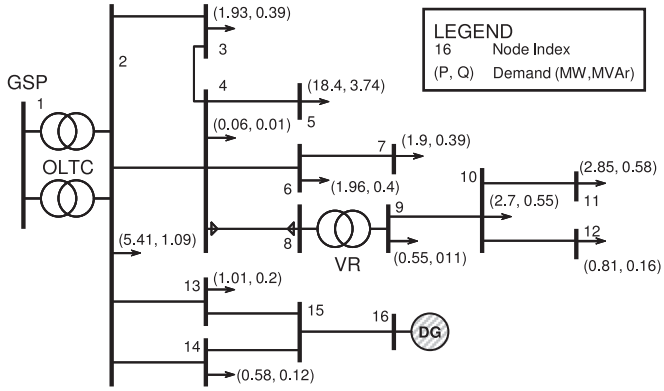

Fig. 5. Simplified UKGDS EHV1–ANM case at full load.

devices that have been aggregated and smoothed to reflect the pattern from medium sized farms. While the sequences of wind and tidal data are not concurrent their independence makes their use of value. The generation time- series has been synchronised into 30-second intervals while the demand pattern was taken at 30-minute intervals. The data was synchronised to run concurrently and linearly interpolated between respective data points to very high resolution time steps in OpenDSS for direct use in the power flow simulations.

A. Simplified EHV1 Network–Single DG

Fig. 5 shows the Simplified EHV1 Network [13], a weakly meshed network of parallel feeders supplied by two 30-MVA 132/33-kV OLTC transformers with a voltage regulator (VR) between buses 8 and 9. Peak network demand is 38.2 MW. A single wind farm is connected at bus 16. The DG reactive power limits are set at 0.98 leading/lagging to mirror the power factor of local load and restrict the circulation of reactive power within the network boundaries. For the 'minimum deviation' OPF three directly and indirectly controlled voltage targets ($V_{b,reg}$) were 1.03pu on buses 2 and 9 and 1.045pu at bus 16. While the directly controlled OLTC voltage settings are continuously penalised, the voltage level on bus 16 is only regulated if the forecast resource level would produce DG output above the firm capacity. Ref. [8] indicates that if the DG is developed as

TABLE I
EHV1-ANM RESULTS SUMMARY

	'fit -and-forget'	Unconstrained	Standard OPF	Min Dev OPF
DG (MW)	3	9	9	9
DG (MWh)	43.01	129.03	129.03	129.03
DG (MVArh)	8.73	26.20	26.20	−26.20
Energy Curtailed (MWh)	0.00	0.00	0.00	0.00
Energy Curtailed (%)	0.0%	0.0%	0.0%	0.0%
Capacity Factor	59.7%	59.7%	59.7%	59.7%
GSP (MWh)	−510.90	−428.72	−429.50	−429.27
GSP (MVArh)	−119.41	−101.26	−103.29	−155.55
GSP power factor	0.974	0.973	0.972	0.940
Network Losses (MWh)	17.8	21.6	22.4	22.1
Network Charge (MVArh)	19.4	18.7	20.7	20.6
Network Losses (%)	3.5%	5.0%	5.2%	5.2%
Minimum Voltage	0.9641	0.9649	0.9434	0.9491
Maximum Voltage	1.0592	1.0933	1.0743	1.0626
Undervoltage Excursion*	0.00%	0.00%	0.00%	0.00%
Overvoltage Excursion*	0.00%	97.92%	27.78%	0.69%
0.00%				
Substat ion Tap Changes	1	1	37	11
VR Tap Changes	12	10	34	12

*Measured in 10-minute averages.

'fit-and-forget' its firm installed capacity would be 3 MW with the DG operating (from the network perspective) at constant 0.98 leading (capacitive) power factor and the substation OLTC and VR target voltages of 1.036 pu and 1.03 pu respectively. By adopting the ANM strategies [8] indicated that the headroom for new DG capacity can be improved. Here, DG capacity was extended to 9-MW.

The network impact and the real-time interactions of the ANM control settings under scheduling from the ANM OPF DDS are assessed for a 24-hour period. The actions and impact of the control schemes are compared with the effect of an unconstrained 9 MW DG (summary statistics in Table I).

A number of metrics were used to demonstrate the quality and effectiveness of the real-time controller: 1) volume of curtailment; 2) total voltage excursion measured as instantaneous peak and 10-minute averages to assess compliance with EN 50160 [14] (which permits short over-voltages <5% of time); 3) exceedance of branch flow limits measured as instantaneous peak relative to rated capacity and as percentage total instantaneous overload over the 24-hour test case; 4) frequency of OLTC taps; 5) the reactive power demand at the Grid Supply Point (GSP, the transmission interface) which may indicate challenges for the transmission system to deliver this [15]. The impact of measurement and communication delays on these metrics are also examined.

1) Energy Yield: As shown in the summary statistics, given in Table I, there was no requirement to curtail real power production of the DG. The net energy yield in both versions of the ANM OPF scheme increased by 200%, in line with capacity increases over the 'fit-and-forget' analysis.

2) Voltage Compliance: Fig. 6 shows the voltage profile for bus 16, the binding constraint on the OPF dispatch. When DG production exceeds the 3-MW firm capacity limit, the voltage level in the unconstrained case is well above statutory limits with a 5-sec instantaneous peak of 1.093pu and 97.9% of 10-min averages.

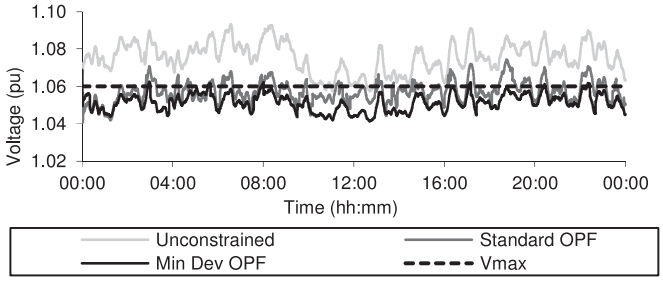

Fig. 6. Simplified EHV1-voltage time series at Bus 16.

At the point of dispatch using the 'standard' ANM OPF scheme, the combination of reactive power management at the DG and the OLTC voltage set-point at the GSP is sufficient to avoid all instances of voltage excursion without recourse to active power curtailment. However, when applied in the network simulation, overvoltages still occur but are substantially reduced in both magnitude and frequency: instantaneous peak overvoltage was 1.074pu and 10-min average overvoltage was observed for 27% of the period.

Overvoltages arise due to fluctuations in DG production between the 5-min control intervals but predominantly due to operating sensitivity as the 'residual' voltage variation within the GSP transformer dead-band. This only becomes evident because of the simulation framework described in Section II-B and underlines the value of the approach in capturing realistic network response should be noted here.

This occurs consistently during periods where the network-wide voltage spread does not extend simultaneously to the upper and lower reaches of the statutory range, meaning there is potential to improve operation by moving network set-points away from voltage limits and operational restrictions.

The 'minimum deviation' objective function improves the network response by prescribing control set-points that are further from network limits, such that residual voltage variation is absorbed within the margins for the operating sensitivity of the network. The results show that overvoltages remain but with 10-min averages reduced to 0.7% and instantaneous peak to 1.063pu, well within the EN50160 requirements. This control strategy has little or no negative impact on the network operation, with the lowest system voltage level at Bus 8 remaining above the minimum limit.

3) Thermal Compliance: Overloading was not experienced as DG production is restricted well below branch capacities with maximum loading of 86% on line 15-16 occurring at peak wind production.

4) Tap Changing: The use of active setting of OLTC and VR voltages results in more tap changes than the unconstrained case. However, the minimum deviation function reduces the number considerably as it relies on DG power factor control: these fell from 37 to 11 and from 34 to 12 at the GSP and VR, respectively (see Fig. 7). A key point is that each OPF control strategy achieves maximum energy yield by favouring a different control asset.

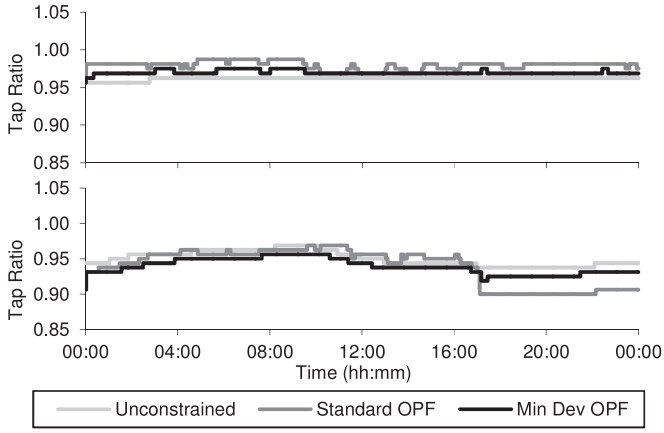

Fig. 7. Tap Positions at the GSP (top) and VR (bottom) transformers.

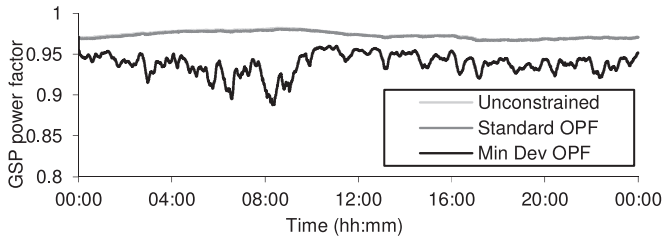

Fig. 8. GSP power factor (n.b. Unconstrained and Standard OPF identical).

5) GSP Reactive Demand: Fig. 8 shows reactive power demand at the GSP. For the standard OPF it slowly changes with active demand, with a profile identical to the unconstrained case. The minimum deviation OPF results in a much more variable, lagging, power factor at the GSP. This falls as low as 0.89 due to greater reliance on DG PF control ahead of OLTC tap changes. In certain cases, this may have further consequences or could possibly be limited by congestion management on the upstream network.

6) Communications Delays: The influence of the 90-second delays between measurement and the OPF decision was examined by setting it to zero and re-running the simulations. Analysis indicated only marginal improvements. In both OPF cases there was no difference in the instantaneous peak voltages experienced with and without the delay; this shows that the most extreme voltage constraints did not result from steady state system conditions. For the standard OPF, removing delays reduced 10-minute average overvoltage excursion by 2.8% to 25%; for the minimum deviation OPF already very low (0.69%) overvoltage excursions were removed entirely.

B. Full EHV1 Network–Multiple DG and Resources

The OPF technique was then evaluated on the Full EHV1 network using multiple DGs and both wind and tidal resources (see Fig. 9). Voltage regulation was consistent with the simplified network with the addition of OLTCs at the 33/11-kV distribution transformers. The full network also contains a 15-MVA interconnector, treated as a PV bus with 1pu target voltage. Prior

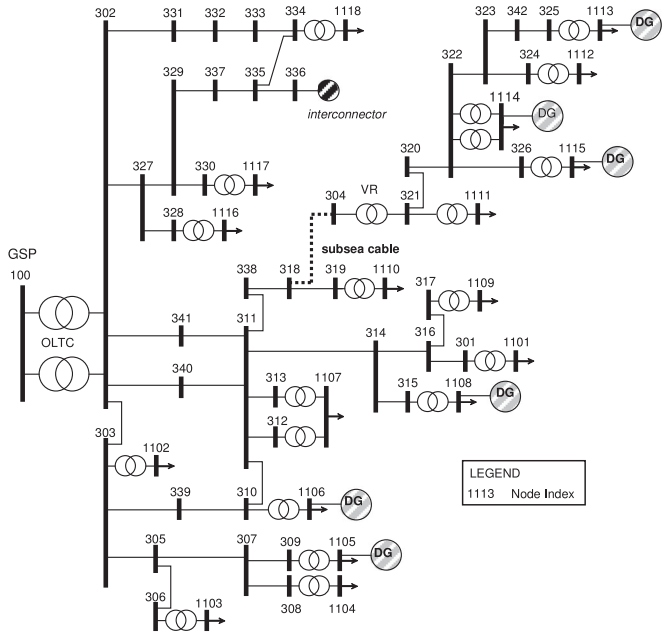

Fig. 9. Full EHV1 network and location of wind and tidal DG [8].

to the connection of DG, the transformer target voltages were 1.045 pu at the substation and 1.03pu at the VR and $33/11-$ kV transformers. In the minimum deviation OPF the internal voltage control targets were 1.02pu for the OLTC and VR transformers, and 1.03pu for the 33/11-kV transformers connected to the DGs. Six DG locations were adopted, with differing renewable energy technologies considered in two geographic zones. On the "mainland", three wind farm developments are considered at buses 1105, 1106, and 1108 (see Fig. 9, bottom left). All three locations are in sufficient proximity to follow the same generation profile. A subsea cable (line 318-304) connects the "mainland" to an "island" on which three tidal generation sites are connected at buses 1113 to 1115 (see Fig. 9, top right) which are also considered to have the same generation pattern.

For the 'fit-and-forget' approach, DG penetration level was limited to 20.5 MW (55% of peak demand) with voltage rise as the binding constraint on DG capacity [8]. Again [8] showed that the number of potential DG locations and their corresponding proximity to loads ANM can enable 52MW of DG with potential generation of 493 MWh over the 24-hour test case. In the work reported in this paper DG was installed with capacities of 5, 15, 10, 2, 10, 10 MW at DG locations 1105-1115 respectively. Sections of the network consequently experience widespread reverse power flows and the active constraint on further DG capacity is a combination of voltage rise and the thermal limits on the 33/11-kV transformers, depending on the supply and demand conditions.

Simulations were conducted over the same 24-hour observation period with the same set of evaluation criteria. Summary results are shown in Table II.

1) Energy Yield: Table II shows that with either ANM control strategy there was only minimal requirement for curtailment of production. In both cases curtailment is 1.25% of the

TABLE II
FULL EHV1 RESULTS SUMMARY

	'fit-and forget'	Unconstrained	Standard OPF	Min Dev OPF
DG (MW)	21	52	52	52
DG (MWh)	236.55	493.16	486.98	486.98
DG (MVArh)	48.03	100.14	6.49	−3.98
Energy Curtailed (MWh)	0.00	0.00	6.18	6.18
Energy Curtailed (%)	0.0%	0.0%	1.3%	1.3%
Capacity Factor	48.1%	39.5%	39.0%	39.0%
GSP (MWh)	−362.68	−129.83	−84.08	−92.57
GSP (MVArh)	−193.92	−132.27	−174.08	−192.85
GSP power factor	0.882	0.700	0.435	0.433
Network Losses (MWh)	16.3	16.7	14.4	14.6
Network Charge (MVArh)	25.6	33.9	33.2	32.7
Network Losses (%)	4.5%	12.9%	17.1%	15.8%
Minimum Voltage	0.9747	0.9738	0.9527	0.9636
Maximum Voltage	1.0510	1.1096	1.0672	1.0703
Undervoltage Excursion*	0.00%	0.00%	0.00%	0.00%
Overvoltage Excursion*	0.00%	96.53%	1.39%	0.00%
Max. Thermal Loading (%)	67.67%	140.10%	119.28%	120.17%
Total overloading	0.00%	24.47%	15.45%	16.34%
Substation Tap Changes	1	0	13	0
VR Tap Changes	19	68	59	47

*Measured in 10-minute averages.

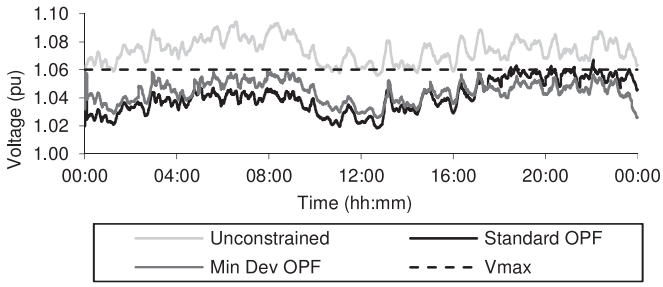

Fig. 10. Voltage at Bus 309 (primary side of transformer 309-1105).

available energy (6.2 MWh of 493 MWh), resulting in an 83.6% increase in yield over the 'fit-and-forget' strategy.

2) Voltage Compliance: In the unconstrained case, the maximum instantaneous voltage level was 1.11pu at Bus 326, where the 10-min average occurrence was 9.2%. However, the worst case overvoltage was at Bus 309, where the occurrence period was 96.5%, with a maximum instantaneous voltage of 1.095pu, as Fig. 10 indicates.

With application of the OPF, instances of voltage rise were significantly reduced with power flows held predominantly within limits. Fig. 10 illustrates the marked reduction in average and peak voltages. Here, the OLTC of the 33/11-kV transformer maintains the voltage target within the target band on the secondary winding, whilst residual voltage variation and short-term DG fluctuation allows the primary winding voltage to climb outside the voltage envelope. For the standard OPF, the maximum instantaneous voltage level was 1.067pu and 10-min overvoltages were only observed for 1.4% on Bus 309, well below the recommended 5% limit. No voltage excursion was evident in the minimum deviation case on a 10-min average basis although

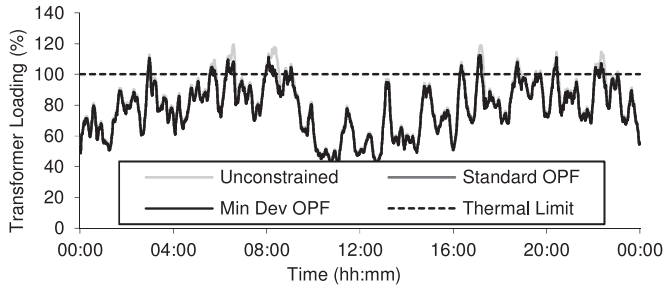

Fig. 11. Loading levels of 33/11-kV transformer 310-1106.

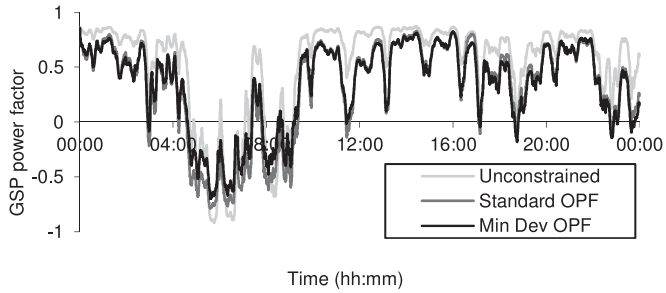

Fig. 12. GSP power factor (+ve = P export; −ve P import).

the maximum instantaneous level reached across all system buses was 1.070pu.

3) Thermal Compliance: Thermal overloading of the network transformers was evident at three 33/11-kV transformers connecting the wind farm DGs (see Fig. 11 shows 310-1106). Overloading of the wind farm 33/11-kV distribution transformers is appreciable. In the unconstrained case overloading peaked in the 309-1105 transformer with a maximum loading level of 140% and an occurrence of 25%.

For the worst affected case (309-1105), maximum instantaneous overloads were 119% and 120% in the standard and minimum deviation cases, respectively, with overall duration of overloads evident for 15% and 16% of the period. Overloading of this magnitude and duration may be acceptable if it occurs only for a certain number of times per year and/or with sufficient recovery time between instances.

4) Tap Changing: Many tap changes occur given the variability. In the unconstrained case 68 tap changes are experienced by the VR and none at the GSP. With the OPF cases the tap changes at the VR drop to 59 and 47, respectively, for the standard and minimum deviation cases. Interestingly, the number of changes at the GSP increases to 13 with the standard OPF but remains at zero for the alternative. This illustrates the different strategies adopted, indicating more reliance on PFC in the minimum deviation case.

5) GSP Reactive Demand: The impact of the control scheduling on the GSP power factor is illustrated in Fig. 12. When the combined real power output from DG is greater than the local network demand, variable PFC strategies import significant levels of reactive power to counteract the large export in real power. However, when demand is greater than generation, there is again a net import of reactive, as well as real power to

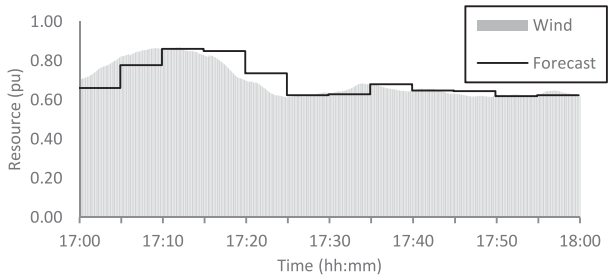

Fig. 13. Example of persistence forecasting routine vs. actual resource data sampling level for wind.

service demand. This means that the network has a sustained reactive power demand (inductive load), while the import/export of real power causes the power factor to vary positive to negative with time. Once again the ability of the transmission network capacity to provide this is an important factor that must be considered when devising a network-wide ANM control scheme. In keeping with the smaller network case, the minimum deviation OPF adopts more extensive use of PFC; in terms of what is seen at the GSP, the effect is masked by the substantially lower individual impact from any one control action and the aggregation of several DG resources.

6) Communications Delays: In the larger network where the optimisation is more constrained by both voltage levels and thermal overloading, the consequences of removing communication delay again is very small. The impact on voltage excursion was negligible with a 0.001 p.u. increase and 0.003 p.u. reduction in the instantaneous peak voltage for the standard and minimum deviation cases respectively. 10-minute average overvoltage excursion was removed entirely. A similar story can be seen with regards to thermal overloading with removal of delays reducing total overloading on each constrained transformer by 1 to 2%. Peak overloading was unaffected.

7) Forecast Error: Overloading and overvoltages are more affected by the fluctuation of resource and demand between the sampling and the 5-minute control intervals, as it departs from the levels implied by the persistence forecast. Fig. 13 shows the real-time and forecasted per-unit wind level for the farm at Bus 1105 over a 1-hour example: here transformer overloading occurs when real-time output exceeds persistence.

Overall the levels of forecast error seen are generally modest. For demand, the mean and maximum absolute errors over the 24-hr test case were 0.21% and 1.22% of winter peak. For wind, the respective values are 3.3% and 18.5% and for tidal they are 0.83% and 11.1%. The perhaps surprising reason for the size of the maximum error for tidal generation is that at the mid-point of the tidal cycle, flow changes are rapid; they are however very predictable and this is a worst case.

While low values of mean absolute forecast error are encouraging, the higher values of maximum forecast error particularly for wind are clearly a challenge. It is encouraging however, that the hierarchical system control (actions are dictated by local infrastructure under guidance of the central OPF dispatch), effectively desensitise the network to some of the effects of forecast errors.

IV. Discussion

The work reported introduces the potential for OPF techniques to schedule active network control set-points in real-time. The application demonstrates the coordination and synchronisation of multiple active control systems and addresses some of the concerns like discontinuous and hysterical switching of system controls and excursion from regulatory power flow regimes. In the Full EHV1 network case study the integration of extremely high DG penetrations fundamentally changes the dynamics and functionality of the network. This cannot be achieved by passive or decentralised control schemes alone. The method has been designed and tested largely on radial distribution networks but it is generic and readily applicable to meshed distribution networks.

The intuitive scaling of the secondary component in the 'minimum deviation' objective function has a near negligible impact on the primary (and standard) objective, and therefore gives similar 'headline' results to the standard OPF in each network case. However, the results are not identical and the contribution of the secondary component in the objective serves (1) to significantly reduce unwarranted (and limited benefit) switching of network set-points between successive control cycles; and (2) to orchestrate voltage levels away from regulatory and operational limits at network nodes particularly sensitive to unavoidable residual voltage variation. The method significantly improves performance, with a reduction in magnitude and frequency of voltage violations and tap-changing actions at the expense of greater reactive power management and reactive power imports from the GSP. What this demonstrates is that broadly the same performance in terms of delivered energy and curtailment is achieved for much lower likelihood of voltage and thermal constraint breaches. Additionally, the minimum deviation term offers potential for the DNO to 'tune' voltage gradients on a seasonal or other basis.

The case study suggests that adverse network impacts from time delays in measurement and communication are relatively modest. Further work is being conducted to consider the deployment of the technique on more coarse timescales alongside embedded decentralised schemes [5], [6] that operate locally and maintain power flows between OPF scheduling points. Application of the technique at higher time resolutions may not be feasible given system communication and control delays and may introduce unwarranted control actuation.

The approach is potentially challenging in terms of the requirements for measurement and communication hardware and associated data flows. However, as DNOs increasingly become responsible for active power flow management in their networks it is problem that is not restricted to this approach. As currently implemented, the control system is fed information on all of the system values. However, one of the advantages of the simulation system is that it can be run using a subset of data to examine the implications and criticality of specific locations to the robustness of the operation. This would require some form of state estimation system to 'fill in the blanks'. This would reduce the volume of information captured as well as reduce hardware requirements but introduces other challenges, not least the

performance of state estimation systems. This is a valuable area for further work as the method is believed to be capable of scaling with uptake of remote measurement systems.

The functioning of the centralised control scheme relies on the availability of the communications infrastructure. It may be feasible to define progressive fail-safe practices to address communications failure that incrementally revert local infrastructure to 'fit-and-forget' set-points and fixing respective ANM control variables in the dispatch until communications can be restored. The control approach appears to be inherently stable; however, enabling substantially more DG may conceivably imply challenges for voltage stability. Further work on these aspects is warranted.

One limitation on the approach is the aggregation and forecasting of power output from renewable energy resources and demand. Persistence forecasting subject to a communications delay, has been used for simplicity. As the test cases show this is not a significant issue for smaller systems but introduces some challenges for larger, more complex systems with high levels of reverse power flow. Deployment at lower time resolutions will require more sophisticated forecasting techniques albeit at greater expense. Work using receding-horizon forecasting techniques is under way to examine its impact on this aspect.

Finally, although this optimisation does not yet consider the implications and limitations posed by commercial arrangements and regulatory incentives, these are important areas of research. The OPF formulation and framework developed are sufficiently flexible to address new constraints associated with principles of access as well as the operation of new technologies such as demand response, energy storage or electric vehicles. However, it should be noted that maximising the value from these technologies require consideration of multiple time frames, not simply sequential snapshot solutions.

V. Conclusion

This work demonstrated a concept for real-time OPF control of DGs and active distribution network assets to maximise the network-wide energy yield in constrained networks. Results clearly show that the ANM OPF technique is capable of real-time scheduling of network control settings and dispatching active and reactive power from renewable DG. The framework for real time simulation highlighted potential complications in deployment, including the residual variation of network operational variables which can induce unwarranted overvoltage excursion and discontinuous switching of network assets in the standard OPF. Customising the OPF algorithm reduced these occurrences by guiding network control settings away from operational boundaries. Adverse network impacts from time delays associated with measurement and communications were found to be relatively modest.

References

[1] P. P. Barker and R. W. De Mello, "Determining the impact of distributed generation on power systems: Part I—Radial distribution systems," in *Proc. IEEE Power Eng. Soc. Summer Meeting*, 2000, pp. 1645–1656.

[2] *Smarter Grids: The Opportunity*, DECC, London, U.K., 2009.

[3] S. Liew and G. Strbac, "Maximising penetration of wind generation in existing distribution networks," *IEE Proc. Gener. Transm. Distrib.*, vol. 149, no. 3, pp. 256–262, 2002.

[4] R. A. Currie, G. W. Ault, R. W. Fordyce, D. F. MacLeman, M. Smith, and J. R. McDonald, "Actively managing wind farm power output," *IEEE Trans. Power Syst.*, vol. 23, no. 3, pp. 1523–1524, Aug. 2008.

[5] A. E. Kiprakis and A. R. Wallace, "Maximising energy capture from DGs in weak networks," *IEE Proc. Gener. Transm. Distrib.*, vol. 151, no. 5, pp. 611–618, 2004.

[6] T. Sansawatt, L. F. Ochoa, and G. P. Harrison, "Smart decentralized control of DG for voltage and thermal constraint management," *IEEE Trans. Power Syst.*, vol. 27, no. 3, pp. 1637–1645, Aug. 2012.

[7] H. Dommel and W. F. Tinney, "Optimal power flow solutions," *IEEE Trans. Power App. Syst.*, vol. PAS-87, no. 10, pp. 1866–1876, Oct. 1968.

[8] L. F. Ochoa, C. J. Dent, and G. P. Harrison, "Distributed network capacity assessment: Variable DG and active networks," *IEEE Trans. Power Syst.*, vol. 25, no. 1, pp. 87–95, Feb. 2010.

[9] T. Boehme, G. P. Harrison, and A. R. Wallace, "Assessment of distribution network limits for non-firm connection of renewable generation," *IET Renew. Power Gener.*, vol. 4, no. 1, pp. 64–74, 2008.

[10] M. J. Dolan, E. M. Davidson, I. Kockar, G. W. Ault, and S. D. J. McArthur, "Distribution power flow management utilizing an online OPF technique," *IEEE Trans. Power Syst.*, vol. 27, no. 2, pp. 790–799, May 2012.

[11] J. G. Robertson, G. P. Harrison, and A. R. Wallace, "A pseudo-real time distribution network simulator for analysis of coordinated ANM control strategies," in *Proc. CIRED Workshop 2012, Integr. Renew. Distrib. Grid*, Lisbon, Portugal, May 29–Jun. 2, 2012.

[12] R. C. Dugan and T. E. McDermott, "An open source platform for collaborating on smart grid research," in *Proc. IEEE Power Eng. Soc. General Meeting*, Detroit, MI, USA, Jul. 24–29, 2011.

[13] Distributed Generation and Sustainable Electrical Energy Centre, United Kingdom Generic Distribution System (UK GDS). [Online]. Available: http://www.sedg.ac.uk/. Accessed on: Feb. 2011.

[14] Power Quality Application Guide, 5.4.2 Voltage Disturbances Standard EN 50160: Voltage Characteristics in Public Distribution Systems, 2004.

[15] A. Keane, L. F. Ochoa, E. Vittal, C. J. Dent, and G. P. Harrison, "Enhanced utilization of voltage control resources with distributed generation," *IEEE Trans. Power Syst.*, vol. 26, no. 1, pp. 252–260, Feb. 2011.

James G. Robertson received the M.Eng. and Ph.D. degrees from the University of Edinburgh, Edinburgh, U.K., in 2010 and 2015, respectively.

He is currently a Research Associate with the University of Edinburgh. His research interests include power systems analysis and the network integration of distributed energy resources.

Gareth P. Harrison (M'02–SM'14) is the Bert Whittington Chair of Electrical Power Engineering with the University of Edinburgh, Edinburgh, U.K. His current research interests include network integration of renewable generation and analysis of the impact of climate change on the electricity industry.

Prof. Harrison is a Chartered Engineer and a Member of the IET.

A. Robin Wallace is currently a Professor of Renewable Energy Systems with the University of Edinburgh, Edinburgh, U.K. and the Director of the U.K. Centre for Marine Energy Research. He is a Consultant on small hydropower and distributed generation issues. His research spans network integration of distributed generation.

Prof. Wallace is a Chartered Engineer, a Fellow of the IET, and a Fellow of the Royal Society of Edinburgh.